第 **1** 段

Only the solutions of the p-polarized waves in both half-spaces are considered here. The electric fields of the p-polarized waves penetrate into the metal ($z < 0$) and dielectric ($z>0$) media, while the magnetic fields are parallel to the interface along the surface ($z = 0$). Along the x axis of the propagating direction, per the notation in Fig. 2.2, the p-polarized plane waves in both half-spaces are written as

$$\begin{pmatrix} \mathbf{E}_i \\ \mathbf{H}_i \end{pmatrix} = \begin{pmatrix} E_{x,d} & 0 & E_{z,d} \\ 0 & H_{y,d} & 0 \end{pmatrix} e^{j(k_{x,i}x-\omega t+k_{z,i}z)}, \qquad (2.3)$$

where $k_{x,i}$ represents the wave vectors within the metal and dielectric media, which are parallel to the interface. Equation (2.3) is expanded into the following forms for a dielectric medium

$$\vec{E}_d(x,z,t) = (E_{x,d}, 0, E_{z,d})\, e^{i(k_{x,d}x+k_{z,d}z-\omega t)}$$

$$\vec{H}_d(x,z,t) = (0, H_{y,d}, 0)\, e^{i(k_{x,d}x+k_{z,d}z-\omega t)} \quad 。$$

(2.4a)

and for a metallic medium

$$\vec{E}_m(x,z,t) = \left(E_{x,m}, 0, E_{z,m}\right) e^{i(k_{x,m}x-k_{z,m}z-\omega t)}$$

$$\vec{H}_m(x,z,t) = (0, H_{y,m}, 0)\, e^{i(k_{x,m}x-k_{z,m}z-\omega t)} \quad 。 \qquad (2.4b)$$

At the interface position of $z = 0$, the continuous boundary conditions of the parallel field component of E_x , H_y , and the wave vectors are

$$\begin{cases} E_{x,d} = E_{x,m} \\ H_{y,d} = H_{y,m} \\ k_{x,d} = k_{x,m} \end{cases} \tag{2.5}$$

--From: “Plasmonic Optics: Theory and Applications” By Yongqian Li, SPIE Press, 2017, p.43-44

SPP的电磁场是具有被约束于金属-电介质界面附近的传输波模式，它的电场强度在垂直的-z方向上迅速倏逝衰减，如图1-6（a）。电场分量$\vec{E}$在金属（$z<0$）和电介质（$z>0$）区域的渗透距离也不同。磁场平行于沿着金属-电介质表面的界面，即在$z=0$平面，则金属和电介质区域，并金属-电介质界面处的电场$\vec{E}$和磁场$\vec{H}$分布分别为：

在$z>0$区域的金属材料部分，电场$\vec{E}_m$和磁场$\vec{H}_m$分别为

$$\vec{E}_m(x,z,t) = \left(E_{x,m}, 0, E_{z,m}\right) e^{i\left(k_{x,m}x - k_{z,m}z - \omega t\right)}$$

$$\vec{H}_m(x,z,t) = (0, H_{y,m}, 0)\, e^{i\left(k_{x,m}x - k_{z,m}z - \omega t\right)} \quad 。 \tag{1-18}$$

在$z<0$区域的电介质部分，电场$\vec{E}_d$和磁场$\vec{H}_d$分别为

$$\vec{E}_d(x,z,t) = \left(E_{x,d}, 0, E_{z,d}\right) e^{i\left(k_{x,d}x + k_{z,d}z - \omega t\right)}$$

$$\vec{H}_d(x,z,t) = (0, H_{y,d}, 0)\, e^{i\left(k_{x,d}x + k_{z,d}z - \omega t\right)} \quad 。 \tag{1-19}$$

在$z=0$金属-电介质界面上，如图 1-6（a），由平行于界面的场分量E_x，H_y的连续边界条件和波矢量$k_{x,n}$的关系，可推导

$$\begin{cases} E_{x,d} = E_{x,m} \\ H_{y,d} = H_{y,m} \\ k_{x,d} = k_{x,m} \end{cases}$$

--来源于：“金属手性微纳结构的非对称传输与圆二色性研究”，吐达洪·阿巴，陕西师范大学，2020 年，第 9-10 页

第 2 段

Figure 2.1 illustrates the behavior of SPPs, which represent both the coupled oscillations of electromagnetic waves and the oscillations of electric charges within the solid medium. The longitudinal surface charge oscillation associated with SPPs results in an electric field component oscillating perpendicular to the metallic–dielectric interface. This electromagnetic field is confined within the vicinity of the interface and decays sharply with the distance away from the interface. In a metallic medium, the SPPs exist in a form of electron fluctuations penetrating into the metal at skin depth. In a dielectric medium, the surface plasmon corresponds to an evanescent wave with a decay length of half of a wavelength of the exciting electromagnetic wave.

--From: “Plasmonic Optics: Theory and Applications” By Yongqian Li, SPIE Press, 2017, p.43-44

如图1-6所示，在入射光束的激发下，金属薄膜与电介质界面形成可以传播的SPPs，图1-6（a）中表示电场强度在金属与电介质界面两边的电场和磁场的空间分布特征。图1-6（b）表示SPP平面波传播衰减的示意图，最强电场主要分布在金属与电介质的界面处，在该界面两边电场强度呈指数衰减，并且在金属薄膜中的衰减率远远快于电介质

中的衰减。图1-6（b）显示电场在金属和电介质中的传播和电场强度的指数衰减。

--来源于："金属手性微纳结构的非对称传输与圆二色性研究"，吐达洪·阿巴，陕西师范大学，2020 年，第 10 页

第 3 段

In the propagation direction along the x axis, the wave vector in the metallic medium equals that in the dielectric material. The curl equation for H in a medium i is

$$\nabla \times \vec{H}_n = \varepsilon_n \frac{\partial \vec{E}_n}{\partial t}。 \tag{2.6}$$

The curl equation can be expanded as

$$(-ik_{z,n}H_{y,n}, 0, ik_{x,n}H_{y,n}) = (-i\omega\varepsilon_n E_{x,n}, 0, -i\omega\varepsilon_n E_{z,n})。 \tag{2.7}$$

where k x,i = 2π/λ is the wave vector component along the x axis in media *i*. The curl equation in Eq. (2.7) is rewritten into the expanded forms of

$$\begin{cases} k_{z,n}H_{y,n} = \varepsilon_n \omega E_{x,n} \\ k_{x,n}H_{y,n} = -\omega\varepsilon_n E_{z,n} \end{cases}。 \tag{2.8}$$

In other words, the curl equations for a dielectric medium are

$$\begin{cases} k_{z,d}H_{y,d} = \omega\varepsilon_d E_{x,d} \\ k_{x,d}H_{y,d} = -\omega\varepsilon_d E_{z,d} \end{cases}。 \tag{2.9}$$

and for a metallic medium

$$\begin{cases} k_{z,m}H_{y,m} = \varepsilon_m \omega E_{x,m} \\ k_{x,m}H_{y,m} = -\omega \varepsilon_m E_{z,m} \end{cases}. \tag{2.10}$$

Based on the continuous boundary conditions [Eq. (2.5)] and the curl equation in the z component [Eq. (2.8a)], the dispersion relation along the interface is

$$k_{z,m}\varepsilon_d = -k_{z,d}\varepsilon_m \tag{2.10}$$

Also from the continuous boundary conditions in Eq. (2.5) and the curl equation in the x component of Eq. (2.8b), the intensity relation of the surface plasmon along the propagation direction is

$$\varepsilon_m E_{z,m} = \varepsilon_d E_{z,d} \tag{2.11}$$

Equations (2.9) and (2.10) are the surface plasmon condition. The exponential decay of the electric fields in their respective half-spaces is

$$E_i \propto \exp(\pm i k_{z,i}) = \exp(\pm z \times k_i). \tag{2.12}$$

The exponential decay of electric fields in two half-spaces is illustrated in Fig. 2.1(b). The following relation remains valid due to the conservation of the wave vectors:

$$k_x{}^2 + k_{z,n}^2 = \varepsilon_n k^2 \tag{2.13}$$

where $k_x = k_{x,d} = \varepsilon k_{x,m}\, k$ and $= \omega/c$. The combination of the dispersion relation [Eq. (2.10)] and Eq. (2.13) leads to the dispersion

relation of the surface plasmon wave propagating at the metal–dielectric interface[9]:

$$\begin{cases} {k_{SPP}}^2 = {k_x}^2 = \frac{\varepsilon_d \varepsilon_m}{\varepsilon_d + \varepsilon_m} k^2 = \frac{\varepsilon_d \varepsilon_m}{\varepsilon_d + \varepsilon_m} (\frac{\omega^2}{c^2}) \\ k_{SPP} = \frac{\omega}{c} \sqrt{\frac{\varepsilon_d \varepsilon_m}{\varepsilon_d + \varepsilon_m}} \end{cases} \quad (2.14)$$

Equation (2.14) remains valid for both real and complex permittivity ε m , i.e., for conductors without and with attenuation. The real part and imaginary part of the dispersion relation [Eq. (2.14)] are expressed as

$$k_{SPP} = k'_{SPP} + ik''_{SPP} = \frac{\omega}{c} \sqrt{\frac{\varepsilon_d \varepsilon_m(\omega)}{\varepsilon_d + \varepsilon_m(\omega)}}。 \quad (2.15)$$

The real and imaginary parts are expanded individually as

$$,\begin{cases} k'_{spp} = \frac{\omega}{c} \sqrt{\frac{\varepsilon_d}{(\varepsilon_1+\varepsilon_d)^2+(\varepsilon_2)^2}} \left(\frac{\varepsilon_e^2+\sqrt{\varepsilon_e^4+(\varepsilon_2\varepsilon_d)^2}}{2} \right)^{\frac{1}{2}} \\ k'_{spp} \frac{\omega}{c} \left(\frac{(\varepsilon_2\varepsilon_d)^2}{2\left(\varepsilon_e^2+\sqrt{\varepsilon_e^4+(\varepsilon_2\varepsilon_d)^2}\right)} \right)^{\frac{1}{2}} \sqrt{\frac{\varepsilon_d}{(\varepsilon_1+\varepsilon_d)^2+(\varepsilon'_m{}^2}} \end{cases}$$

(2.16a)

where $\varepsilon_e^2 = (\varepsilon_1)^2 + (\varepsilon_2)^2 + \varepsilon_d \varepsilon_1$. For noble metals, the conditions are satis-fied in the visible light and infrared region, $\varepsilon_1 < 0, |\varepsilon_1| > \varepsilon_{real-dielectric}$ and $|\varepsilon_1| >> \varepsilon_2$ equation (2.16) is thus simplified as

$$\begin{cases} k'_{spp} = \frac{\omega}{c} \sqrt{\frac{\varepsilon_1 \varepsilon_d}{\varepsilon_1+\varepsilon_d}} \\ k'_{spp} \frac{1\omega\varepsilon_1 m \varepsilon_d^{\frac{3}{2}}}{2\,c\,\varepsilon_1+\varepsilon_d} \frac{\varepsilon_2}{(\varepsilon_1)^2} \end{cases}。 \quad (2.17b)$$

The imaginary part of the dielectric functions leads to a damping propagation of SPPs along the interface. When the imaginary parts $k'_{SPP} >> k''_{SPP}$ of the complex dispersion relation in Eq. (2.17b) are assumed to be small compared with the real parts k_{0x}, the damping contribution can be ignored.

--From: "Plasmonic Optics: Theory and Applications" By Yongqian Li, SPIE Press, 2017, p.44-46

从以上表达式可以看出，沿着在 x 轴的传播方向上，金属膜中的波矢量等于介质中的波矢，即$k_x = k_{x,d} = k_{x,m}$。同时。$\vec{H}$在介质中的旋度方程为

$$\nabla \times \vec{H}_n = \varepsilon_n \frac{\partial \vec{E}_n}{\partial t}。 \tag{1-21}$$

方程（1-21）跟（1-20）结合，可以扩展表示为

$$(-ik_{z,n}H_{y,n}, 0, ik_{x,n}H_{y,n}) = (-i\omega\varepsilon_n E_{x,n}, 0, -i\omega\varepsilon_n E_{z,n})。 \tag{1-22}$$

这里，$k_{x,n} = 2\pi/\lambda_n$是在 n 介质中沿着 x 轴的分波矢量。整理表达式（1-22）可得到以下的方程组，

$$\begin{cases} k_{z,n}H_{y,n} = \varepsilon_n \omega E_{x,n} \\ k_{x,n}H_{y,n} = -\omega\varepsilon_n E_{z,n} \end{cases}。 \tag{1-23}$$

则对于金属区域而言，由方程组(1-23)中，可以推导金属区域内的关系为，

$$\begin{cases} k_{z,m}H_{y,m} = \varepsilon_m \omega E_{x,m} \\ k_{x,m}H_{y,m} = -\omega \varepsilon_m E_{z,m} \end{cases}。 \tag{1-24}$$

对于电介质区域而言，同样由方程组（1-23）可以写为电介质中的关系。即，

$$\begin{cases} k_{z,d}H_{y,d} = \omega \varepsilon_d E_{x,d} \\ k_{x,d}H_{y,d} = -\omega \varepsilon_d E_{z,d} \end{cases}。 \tag{1-25}$$

根据边界条件方程组（1-12）、（1-16）和（1-17）表达式联立，可得沿着金属-介质之间的界面的 SPP 波的色散关系可表示为

$$k_{z,m}\varepsilon_d = -k_{z,d}\varepsilon_m。 \tag{1-26}$$

同理，沿金属-电介质之间的界面处的电场强度关系，可以表示为

$$\varepsilon_m E_{z,m} = \varepsilon_d E_{z,d}。 \tag{1-27}$$

由于波矢量守恒，它们的关系是可以表示为

$$k_x{}^2 + k_{z,n}^2 = \varepsilon_n k^2, \tag{1-28}$$

其中，$k_x = k_{x,d} = \varepsilon k_{x,m}$和$k = \omega/c$。由式(1-26)和(1-27)可以推出金属-电介质界面传播的 SPP 的波矢量k_{SPP}

$$\begin{cases} k_{SPP}{}^2 = k_x{}^2 = \frac{\varepsilon_d \varepsilon_m}{\varepsilon_d + \varepsilon_m} k^2 = \frac{\varepsilon_d \varepsilon_m}{\varepsilon_d + \varepsilon_m} (\frac{\omega^2}{c^2}) \\ k_{SPP} = \frac{\omega}{c} \sqrt{\frac{\varepsilon_d \varepsilon_m}{\varepsilon_d + \varepsilon_m}} \end{cases} \tag{1-29}$$

其中 *kx* 表示 SPPs 在 *x* 方向上的波矢量。方程组（1-29）对金属的复介电函数$\varepsilon_m = \varepsilon_1 + i\varepsilon_2$的实部和虚部都成立。

$$k_{SPP} = k'_{SPP} + ik''_{SPP} = \frac{\omega}{c}\sqrt{\frac{\varepsilon_d \varepsilon_m(\omega)}{\varepsilon_d + \varepsilon_m(\omega)}}。 \quad (1\text{-}30)$$

SPP 平面波的波矢量k_{SPP}的实部和虚部分别为

$$\begin{cases} k'_{spp} = \frac{\omega}{c}\sqrt{\frac{\varepsilon_d}{(\varepsilon_1+\varepsilon_d)^2+(\varepsilon_2)^2}}\left(\frac{\varepsilon_e^2+\sqrt{\varepsilon_e^4+(\varepsilon_2\varepsilon_d)^2}}{2}\right)^{\frac{1}{2}} \\ k'_{spp}\frac{\omega}{c}\left(\frac{(\varepsilon_2\varepsilon_d)^2}{2\left(\varepsilon_e^2+\sqrt{\varepsilon_e^4+(\varepsilon_2\varepsilon_d)^2}\right)}\right)^{\frac{1}{2}}\sqrt{\frac{\varepsilon_d}{(\varepsilon_1+\varepsilon_d)^2+(\varepsilon'_m{}^2}} \end{cases}, \quad (1\text{-}31)$$

其中，$\varepsilon_e^2 = (\varepsilon_1)^2 + (\varepsilon_2)^2 + \varepsilon_d\varepsilon_1$。一般来讲，金属薄膜的介电常数与入射电磁波的波长密切相关，是入射电磁波频率的函数。根据 Drude-Lorentz 金属材料的色散模型，金属材料只在可见光和红外波段满足此条件，$\varepsilon_1 < 0, |\varepsilon_1| > \varepsilon_{real-dielectric}$和$|\varepsilon_1| >> \varepsilon_2$，则 SPP 的波矢量满足

$$\begin{cases} k'_{spp} = \frac{\omega}{c}\sqrt{\frac{\varepsilon_1\varepsilon_d}{\varepsilon_1+\varepsilon_d}} \\ k'_{spp}\frac{1\omega\varepsilon_1{}_m\varepsilon_d^{\frac{3}{2}}}{2\,c\;\varepsilon_1+\varepsilon_d}\frac{\varepsilon_2}{(\varepsilon_1)^2} \end{cases}。 \quad (1\text{-}32)$$

因为 SPP 波矢量的实部远远大于虚部，即$k'_{SPP} >> k''_{SPP}$，因此，k''_{SPP}对 SPP 平面波的作用很小，通常把它忽略不计。

--来源于："金属手性微纳结构的非对称传输与圆二色性研究"，吐达洪·阿巴，陕西师范大学，2020 年，第 10-11 页

第 4 段

The propagation of SPPs suffers from the damping contribution from both free and bound electrons. Therefore, the dielectric permittivity is complex, and the traveling SPPs are damped with an energy attenuation. 12 There are three characteristic length scales associated with a surface plasmon: the propagation length, the SPP wavelength, and the penetration depth of the electromagnetic field associated with the SPP mode (in the dielectric medium and in the metal). These characteristic lengths associated with SPPs are demonstrated in Fig. 2.6(a).

The nonlocal dispersive response of metals provides a lower limit of a few nanometers, whereas the propagation length of long-range SPPs reaches up to tens of centimeters. The typical decay length in dielectric media is on the order of hundreds of nanometers, which is less than half of the wavelength of the incident electromagnetic wave. However, the decay length of metals features tens of nanometers, which is two orders of magnitude smaller than the wavelength. Obviously, the SPP propagation lengths span seven orders of magnitude from a few nanometers to tens of centimeters.

Figure 2.6(b) shows the SPP propagation lengths of two typical metals (silver and aluminum). The SPP feature lengths offer the potential for subwave length plasmonic optics. Above all, the penetration lengths in

metals, which are far less than the wavelength, determine the minimum sizes that can be used in plasmonic devices.

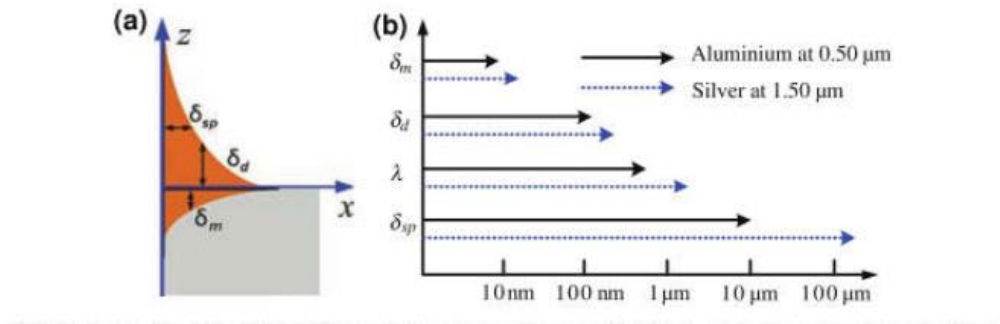

Figure 2.6 (a) Characteristic lengths associated with SPPs. (b) Example of the SPP propagation characteristics of silver and aluminum.

--From: "Plasmonic Optics: Theory and Applications" By Yongqian Li, SPIE Press, 2017, p.51

了解 SPP 平面电磁波在空间的分布和传播特征后，就可以讨论 SPP 的在金属和电介质中的各种特征长度，这就可以更好的理解 SPP 的特性。如图 1-7(b,c)所示，SPP 在两种界面处传播时，会有四个特征长度，它们分别是 SPP 的传播长度δ_{SPP}，SPP 波的波长λ_{spp}，与 SPP 平面波有关的电磁场穿透进电介质材料中的深度δ_d和电磁场穿透进金属中的深度δ_m。为了更好的解释这四个特征长度，在图 1-7 呈现了 SPP 在金属-电介质界面传播时，银和铝两种贵金属材料的四个特征长度对比，从四个不同长度的数量级大小可以看出，$\delta_{SPP} > \lambda_{spp} > \delta_d > \delta_d$，并且在同样的条件下，SPP 波的四个特征长度，在银（Ag）和铝（Al）中的相对长度也不一样。在银金属材料中的穿透深度比铝中的穿透深度更深。

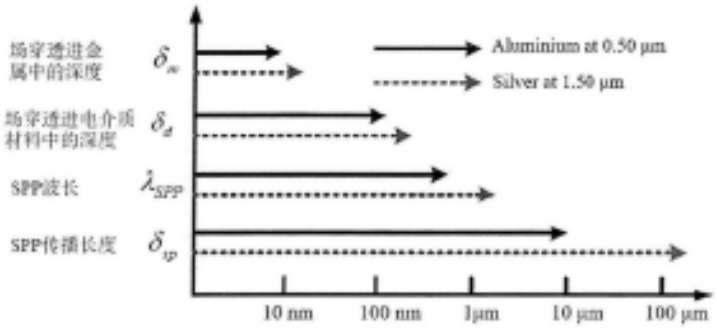

图 1-7金属-介质界面附近SPPs的四种特征尺度[44, 45]。

Fig. 1-7 Four characteristic scale of SPPs propagating at metal-medium interface.

--来源于：“金属手性微纳结构的非对称传输与圆二色性研究”，吐达洪·阿巴，陕西师范大学，2020 年，第 11-12 页

第 5 段

The wavelength of SPPs is the period of the surface charge density oscillation.

The surface plasmon wavelength can be found from the real part of the complex dispersion relation [Eq. (2.14) or Eq. (2.17a)]:

$$k'_{SPP} = \frac{\omega}{c}\sqrt{\frac{\varepsilon_1\varepsilon_d}{\varepsilon_1+\varepsilon_d}} \tag{2.33}$$

The surface plasmon wavelength is then

$$\lambda_{SPP} = \frac{2\pi}{k'_{SPP}} = \lambda_0\sqrt{\frac{\varepsilon_d+\varepsilon_1}{\varepsilon_d\varepsilon_1}} \tag{2.34}$$

Figure 2.7 gives the surface plasmon wavelengths of two typical metals. It is obvious that the propagation wavelengths are always less than the wavelength in free space. During the calculation of these data, the radiative damping was neglected. The relative permittivity of the associated dielectric medium was taken to be one unit.

--From: "Plasmonic Optics: Theory and Applications" By Yongqian Li, SPIE Press, 2017, p.51-52

这四个特征长度由以上的SPP的波矢量表达式可推导出，即SPP的波长是表面电荷密度振荡的周期，因此SPP的振荡波长，式(1-29)和(1-32)中的复色散关系的实部关系式可得到，

$$k'_{SPP} = \frac{\omega}{c}\sqrt{\frac{\varepsilon_1\varepsilon_d}{\varepsilon_1+\varepsilon_d}}。 \tag{1-33}$$

根据等式$\lambda_{SPP} = 2\pi/k'_{SPP}$，则 SPP 的波长为

$$\lambda_{SPP} = \frac{2\pi}{k'_{SPP}} = \lambda_0\sqrt{\frac{\varepsilon_d+\varepsilon_1}{\varepsilon_d\varepsilon_1}}, \tag{1-34}$$

其中，k'_{SPP}，ε_1分别是 SPP 波矢量的实部和金属复介电函数的实部。表达式(1-34)中可见，SPP 波的波长λ_{SPP}总是小于真空中的入射电磁波的波长λ_0。

--来源于："金属手性微纳结构的非对称传输与圆二色性研究"，吐达洪·阿巴，陕西师范大学，2020 年，第 12 页

第 6 段

The propagation length of SPPs indicates the concentration of the wave energy in the vicinity of the interface. The surface plasmon propagation length is defined as the distance over which the power or intensity of the SPPs falls to 1/e of its original value. It can be estimated from the complex dispersion relation expressed in Eq. (2.17b) as

$$\delta_{sp} = \frac{1}{|2k_x''|}, k_x'' = k_0 \frac{\varepsilon_m''}{2(\varepsilon_m')^2} \left(\frac{\varepsilon_d \varepsilon_m'}{\varepsilon_d + \varepsilon_m'} \right)^{3/2}. \quad (2.36)$$

When the metallic medium is low loss, and in the case of $|\varepsilon_1| >> \varepsilon_d$, the propagation length is approximated

$$\delta_{SPP} \approx \lambda_0 \frac{(\varepsilon_1)^2}{2\pi(\varepsilon_2)}。 \quad : (2.37)$$

Equation (2.37) implies that the conditions of a larger real part and a small imaginary part of the dielectric permittivity for a metallic medium promise a longer propagation length.

--From: “Plasmonic Optics: Theory and Applications” By Yongqian Li, SPIE Press, 2017, p.52-53

如果在金属表面上设计各种周期调节结构以实现对 SPP 的控制，那么这时结构周期必须与λ_{SPP}同一量级。

$$k'_{SPP}\frac{\omega}{c}\left(\frac{\varepsilon_1\varepsilon_d}{\varepsilon_1+\varepsilon_d}\right)^{\frac{3}{2}}\frac{\varepsilon_2}{2(\varepsilon_1)^2}。\quad (1\text{-}35)$$

根据表达式(1-32)，SPP的传播长度δ_{SPP}主要取决于SPP波矢的虚部，即当低损耗性金属材料作时，在$|\varepsilon_1| >> \varepsilon_d$情况下，SPP的传播长度近似表示为

$$\delta_{SPP} \approx \lambda_0 \frac{(\varepsilon_1)^2}{2\pi(\varepsilon_2)}。\quad (1\text{-}36)$$

这说明，SPP 的传播长度δ_{SPP}决定了 SPP 元件和回路的最大尺寸的上限。

--来源于："金属手性微纳结构的非对称传输与圆二色性研究"，吐达洪·阿巴，陕西师范大学，2020 年，第 12 页

第 7 段

The penetration depths can be found from the wave vector of the surface plasmon. As mentioned in Chapter 1, the penetration depths d_i in the dielectric and the metal are defined as the reciprocal wave vector

$$\delta_m = \frac{1}{|k_{z,m}|}, (n = d, m) \quad (2.38)$$

over which the electric fields in a metallic or dielectric medium fall to 1/e. The penetration depths from the dispersion relation Eq. (2.19) in a metallic medium with permittivity ε m and a dielectric medium with permittivity δ_d are δ_m

$$\begin{cases}\delta_d = \frac{1}{k_0}\sqrt{\frac{\varepsilon'_m+\varepsilon_d}{\varepsilon_d^2}} = \frac{\lambda_0}{2\pi}\sqrt{\frac{\varepsilon'_m+\varepsilon_d}{\varepsilon_d^2}} \\ \delta_m = \frac{1}{k_0}\sqrt{\frac{\varepsilon'_m+\varepsilon_d}{(\varepsilon'_m)^2}} = \frac{\lambda_0}{2\pi}\sqrt{\frac{\varepsilon'_m+\varepsilon_d}{(\varepsilon'_m)^2}}\end{cases} \tag{2.39b}$$

The penetration depths into metals and dielectric media are estimated by Eq. (2.39), as shown in Fig. 2.9.

--From: "Plasmonic Optics: Theory and Applications" By Yongqian Li, SPIE Press, 2017, p.54

当考虑到由金属-介质交界面构成的无限大平面时，SPP 波在金属中的穿透深度可$\delta_m = \frac{1}{|k_{z,m}|}, (n = d, m)$，根据表达式（1-25）可以推导出 SPP 波穿透入介质的深度δ_d和穿透入金属中的深度δ_m为

$$\begin{cases}\delta_d = \frac{1}{k_0}\sqrt{\frac{\varepsilon'_m+\varepsilon_d}{\varepsilon_d^2}} = \frac{\lambda_0}{2\pi}\sqrt{\frac{\varepsilon'_m+\varepsilon_d}{\varepsilon_d^2}} \\ \delta_m = \frac{1}{k_0}\sqrt{\frac{\varepsilon'_m+\varepsilon_d}{(\varepsilon'_m)^2}} = \frac{\lambda_0}{2\pi}\sqrt{\frac{\varepsilon'_m+\varepsilon_d}{(\varepsilon'_m)^2}}\end{cases}。 \tag{1-37}$$

以上的内容是表面等离激元里面的SPP波的基本传播方式和空间分布原理，它为本文的理论研究提供了科学的理论依据。

--来源于："金属手性微纳结构的非对称传输与圆二色性研究"，吐达洪·阿巴，陕西师范大学，2020 年，第 12-13 页

第 **8** 段

When the dimensional size of a particle is much smaller than the wavelength of the electromagnetic field, their interaction can be analyzed using the quasi-static approximation, 8 whereby the spatial field

distribution around a particle can be considered as an electrostatic field over the particle volume. This approximation describes adequately the electromagnetic response of nanoparticles with dimensional sizes less than 100 nm .

--From: “Plasmonic Optics: Theory and Applications” By Yongqian Li, SPIE Press, 2017, p.69

假设，金属纳米颗粒球的尺寸远远小于入射光波的波长（$d << \lambda$），光与金属纳米颗粒之间的相互作用可以看作准静态近似法来分析，则可以将金属纳米颗粒周围的空间场分布视为金属纳米颗粒体积上的准静电场[50, 51]。通常，用准静态近似法能够完全充分描述尺寸小于 100 nm 以下的金属纳米颗粒。

--来源于：“金属手性微纳结构的非对称传输与圆二色性研究”，吐达洪·阿巴，陕西师范大学，2020 年，第 14 页

第 9 段

In the quasi-static approximation, the electric field is represented by a potential as $\vec{E}_{in} = -\nabla\Phi$ The potential satisfies the Laplace equation $\nabla^2\Phi = 0$ 8 As show in Fig. 3.4(b), the Laplace equation in spherical coordinates $(r, \theta, \varphi)$is

$$\nabla^2(r,\theta,\varphi) \times r^2 \sin\theta = \sin\theta \frac{\partial}{\partial}\left(r^2 \frac{\partial}{\partial r}\right) + \frac{\partial}{\partial\theta}\left(\sin\theta \frac{\partial}{\partial\theta}\right) + \frac{1}{\sin\theta}\frac{\partial^2}{\partial^2\varphi} \tag{3.1}$$

where r, u, and f are the radius, polar angle, and azimuthal angle in polar coordinates.

--From: “Plasmonic Optics: Theory and Applications” By Yongqian Li, SPIE Press, 2017, p.70

在外电场作用下，纳米球颗粒由于电偶极子激发，该金属纳米颗粒具有均匀的极化，因此，可以通过简单的静电场理论来分析金属纳米颗粒体积上的空间场分布。当满足静电近似条件时，则在入射光波的照射下，金属纳米颗粒球附近的电场，可以由电场电势$\vec{E}_{in} = -\nabla\Phi$来表示，电场电势满足拉普拉斯方程$\nabla^2\Phi = 0$。如图 1-9（b）所示，在球坐标系下，拉普拉斯方程在球坐标(r, θ, φ)中的表达式为[52]

$$\nabla^2(r,\theta,\varphi) \times r^2 \sin\theta = \sin\theta \frac{\partial}{\partial}\left(r^2 \frac{\partial}{\partial r}\right) + \frac{\partial}{\partial\theta}\left(\sin\theta \frac{\partial}{\partial\theta}\right) + \frac{1}{\sin\theta}\frac{\partial^2}{\partial^2\varphi} \quad (1\text{-}38)$$

其中，r是球坐标的半径，θ是极角，ϕ是方位角。

--来源于：“金属手性微纳结构的非对称传输与圆二色性研究”，吐达洪·阿巴，陕西师范大学，2020 年，第 14-15 页

第 10 段

At an infinite distance away from the sphere $r \to \infty$, the requirement of $\Phi_d = -E_{in} r \cos\theta$rcosu gives rise to $B = -E_{in}$.

At the surface r¼ d, the tangential electric field and the normal

component of the electric potential demands the boundary conditions

$$\begin{cases} \dfrac{\partial \Phi_d(r,\theta)}{\partial \theta} = \dfrac{\partial \Phi_m(r,\theta)}{\partial \theta} \\ \varepsilon_d \dfrac{\partial \Phi_d(r,\theta)}{\partial r} = \varepsilon_m \dfrac{\partial \Phi_m(r,\theta)}{\partial r} \end{cases}$$

The incoming electric field is assumed to be homogeneous and propagate along the x axis$\Phi \ = -E_x = -E \ r\cos\theta$. The evaluation of the boundary conditions leads to the potentials Φ_m inside the metallic sphere and Φ_d within the dielectric medium

$$\begin{cases} \Phi_m(r,\theta) = E_{in}\dfrac{3\varepsilon_d}{\varepsilon_m + 2\varepsilon_d} r\cos\theta \\ \Phi_d(r,\theta) = -E_{in} r\cos\theta + E_{in}\dfrac{\varepsilon_m - \varepsilon_d}{\varepsilon_m + 2\varepsilon_d}\left(\dfrac{d}{r}\right)^2 r\cos\theta \end{cases}$$

--From: “Plasmonic Optics: Theory and Applications” By Yongqian Li, SPIE Press, 2017, p.71

当球坐标半径趋向于无穷大时$r \to \infty$，在电介质中的电势表达式为$\Phi_d = -E_{in} r\cos\theta$，则可以推导出$B = -E_{in}$。在金纳米颗粒球表面处，即$r = d$，切向电场和电势的法向分量满足边界条件，即

$$\begin{cases} \dfrac{\partial \Phi_d(r,\theta)}{\partial \theta} = \dfrac{\partial \Phi_m(r,\theta)}{\partial \theta} \\ \varepsilon_d \dfrac{\partial \Phi_d(r,\theta)}{\partial r} = \varepsilon_m \dfrac{\partial \Phi_m(r,\theta)}{\partial r} \end{cases}^{\circ} \qquad (1\text{-}39)$$

边界条件相对于激发电场的极化具有轴向对称性，并且它跟激发电场与方位角ϕ无关。

假定入射电场E_{in}是均匀的并沿 x 轴传播且满足$\Phi \ = -E_x =$

$-E\ \ r\cos\theta$，当对称轴为 z 轴时，边界条件分别引起在金属纳米球内部电势Φ_m和电介质内电势Φ_d，则它们表示为

$$\begin{cases}\Phi_m(r,\theta)=E_{in}\frac{3\varepsilon_d}{\varepsilon_m+2\varepsilon_d}r\cos\theta\\ \Phi_d(r,\theta)=-E_{in}r\cos\theta+E_{in}\frac{\varepsilon_m-\varepsilon_d}{\varepsilon_m+2\varepsilon_d}(\frac{d}{r})^2r\cos\theta\end{cases} \quad (1\text{-}40)$$

--来源于："金属手性微纳结构的非对称传输与圆二色性研究"，吐达洪·阿巴，陕西师范大学，2020 年，第 15 页

第 **11** 段

Following the vector relationship $\vec{E}_{in}=-\nabla\Phi$, Eqs. (3.5) give rise to the electric fields inside and outside the nanoparticle:

$$\vec{E}_m(r,\theta)=\frac{3\varepsilon_d}{\varepsilon_m+2\varepsilon_d}\vec{E}_{in}r\cos\theta, \quad (1\text{-}41)$$

$$\vec{E}_d(r,\theta)=\vec{E}_{in}r\cos\theta+\frac{\varepsilon_m-\varepsilon_d}{\varepsilon_m+2\varepsilon_d}(\frac{d}{r})^3\vec{E}_{in}[r\cos\theta-3\cos\theta(\sin\theta+\cos\theta)]$$

。

--From: "Plasmonic Optics: Theory and Applications" By Yongqian Li, SPIE Press, 2017, p.72

将等式$\vec{E}_{in}=-\nabla\Phi$代入表达式(1-40)，则金属纳米颗粒球内部($\vec{E}_m$)和外部（$\vec{E}_d$）的电场分布分别为

$$\vec{E}_m(r,\theta)=\frac{3\varepsilon_d}{\varepsilon_m+2\varepsilon_d}\vec{E}_{in}r\cos\theta, \quad (1\text{-}41)$$

$$\vec{E}_d(r,\theta)=\vec{E}_{in}r\cos\theta+\frac{\varepsilon_m-\varepsilon_d}{\varepsilon_m+2\varepsilon_d}(\frac{d}{r})^3\vec{E}_{in}[r\cos\theta-3\cos\theta(\sin\theta+$$

$cos\,\theta)]$

。 （1-42）

--来源于：“金属手性微纳结构的非对称传输与圆二色性研究”，吐达洪·阿巴，陕西师范大学，2020 年，第 15 页

第 **12** 段

The second term in Eqs. (3.6b) and (3.7b) describes the scattering field distribution. The scattering field looks identical to the oscillating field of a dipole locating at the origin position. The dipole moment p is defined as

$$p = 4\pi\varepsilon_m d^3 \frac{\varepsilon_m - 2\varepsilon_d}{\varepsilon_m + 2\varepsilon_d} E_{in}$$

The polarizability χ_m of the dipole p= εd χ_d E0 induced by the external field E0 is defined as

$$\chi_m = 4\pi d^3 \frac{\varepsilon_m - 2\varepsilon_d}{\varepsilon_m + 2\varepsilon_d}$$

--From: “Plasmonic Optics: Theory and Applications” By Yongqian Li, SPIE Press, 2017, p.72-73

同样按照表达式(1-40)，可推导出金属纳米球的电偶极矩（p）表达式

$$p = 4\pi\varepsilon_m d^3 \frac{\varepsilon_m - 2\varepsilon_d}{\varepsilon_m + 2\varepsilon_d} E_{in}。 \quad (1\text{-}43)$$

这时，金属纳米球的共振增强极化率（χ_m）可以写为

$$\chi_m = 4\pi d^3 \frac{\varepsilon_m - 2\varepsilon_d}{\varepsilon_m + 2\varepsilon_d}。 \quad (1\text{-}44)$$

依据表达式（1-44）可知，显然，当$|\varepsilon_m + 2\varepsilon_d|$取最小值时，即$|\varepsilon_m = -2\varepsilon_d|$时，极化率$\chi_m$达到最大值。

--来源于："金属手性微纳结构的非对称传输与圆二色性研究"，吐达洪·阿巴，陕西师范大学，2020 年，第 15-16 页

第 **13** 段

The polarizability x_m would satisfy the resonance condition when the term ε m þ 2ε d reaches its minimum value. The imaginary part Im(ε m) of most noble metals is very small and has slowly varying values with respect to the ent is simplified to

$$Re(\varepsilon_m) = -2\varepsilon_d$$

If the permittivity of the metallic media satisfies roughly the resonance condition, then Eqs. (3.6) and (3.7) indicate that the electric fields inside and outside the nanoparticle are enhanced relative to the incident field.

--From: "Plasmonic Optics: Theory and Applications" By Yongqian Li, SPIE Press, 2017, p.73

依据表达式（1-44）可知，显然，当$|\varepsilon_m + 2\varepsilon_d|$取最小值时，即$|\varepsilon_m = -2\varepsilon_d|$时，极化率$\chi_m$达到最大值。通常情况下，绝大多数金属介电常数的虚部 Im（ε_m）很小，相比于实部，它的变化也可以忽略不记。在这种情况下，金属纳米球材料发生表面局域共振的条件是

$$Re(\varepsilon_m) = -2\varepsilon_d \tag{1-45}$$

根据(1-41)和(1-42)表达式，相对于入射电场E_{in}，金属纳米球颗粒内部电场 ($\vec{E}_m$) 和外部电场 ($\vec{E}_d$) 的都有明显增强了。从光学的角度看，共振增强极化率χ_m的另一个贡献在于对金属纳米颗粒的光散射和光吸收的增强

--来源于：“金属手性微纳结构的非对称传输与圆二色性研究”，吐达洪·阿巴，陕西师范大学，2020 年，第 15-16 页

第 **14** 段

The extinction efficiency is the sum of scattering efficiency σ_{sca} and absorption efficiency σ_{abs}

$$\sigma_{ext} = \sigma_{abs} + \sigma_{sca}$$

--From: “Plasmonic Optics: Theory and Applications” By Yongqian Li, SPIE Press, 2017, p.76-77

因为消光系数为$\sigma_{ext} = \sigma_{abs} + \sigma_{sca}$，复介电函数$\varepsilon_m(\omega) = \varepsilon_1(\omega) + i\varepsilon_2(\omega)$，因此，相应的消光系数为

--来源于：“金属手性微纳结构的非对称传输与圆二色性研究”，吐达洪·阿巴，陕西师范大学，2020 年，第 16 页

第 **15** 段

Based on the polarizability of metal spherical particles in Eq. (3.9), the

scattering coefficiency is obtained by dividing the total radiated power of the exciting wave:

$$\sigma_{sca} = \frac{k_d^4}{6\pi\varepsilon_0}|\chi_m(\omega)|^2 = \frac{8\pi}{3}k_d^4R^6\left|\frac{\varepsilon_m(\omega)-\varepsilon_d}{\varepsilon_m(\omega)+2\varepsilon_d}\right|^2 \quad (3.21a)$$

$$\sigma_{abs} = k_d\, Im\,|\chi_m(\omega)| = 4\pi k_d R^3\, Im\left[\frac{\varepsilon_m(\omega)-\varepsilon_d}{\varepsilon_m(\omega)+2\varepsilon_d}\right] \quad (3.21b)$$

--From: “Plasmonic Optics: Theory and Applications” By Yongqian Li, SPIE Press, 2017, p.79

由（1-44）中，可得到金属球形纳米粒子的极化率。则对应的散射截面（散射系数σ_{sca}）和吸收率（吸收系数σ_{abs}）分别表示为[53,54]

$$\sigma_{sca} = \frac{k_d^4}{6\pi\varepsilon_0}|\chi_m(\omega)|^2 = \frac{8\pi}{3}k_d^4R^6\left|\frac{\varepsilon_m(\omega)-\varepsilon_d}{\varepsilon_m(\omega)+2\varepsilon_d}\right|^2, \quad (1\text{-}46)$$

$$\sigma_{abs} = k_d\, Im\,|\chi_m(\omega)| = 4\pi k_d R^3\, Im\left[\frac{\varepsilon_m(\omega)-\varepsilon_d}{\varepsilon_m(\omega)+2\varepsilon_d}\right], \quad (1\text{-}47)$$

方程（1-46）和（1-47）表明，在产生局域表面等离激元条件下，金属球形纳米粒子吸收和散射都是被因LSP共振而得到增强。当金属纳米颗粒的吸收和散射满足条件（1-45）时，金属球形纳米粒子附近产生强烈电偶极子共振，使它的吸收和散射增强。

--来源于：“金属手性微纳结构的非对称传输与圆二色性研究”，吐达洪·阿巴，陕西师范大学，2020 年，第 16 页

第 16 段

Equation (3.20) indicates that the resonance condition $\varepsilon_1(\omega) =$

$-\chi\varepsilon_d(\omega)$ remains valid if the imaginary part $\varepsilon''(\omega)$ is weakly dependent on frequency. The factor x equals 2 for the case ofa sphere with a small radius. The value of factor x can only be solved analytically for spheres and spheroids. It often approximates 3 for ellipsoid particles. When $\varepsilon_1(\omega) = -2\varepsilon_d(\omega)$and $\varepsilon''(\omega)$are independent of the frequency, a small sphere reaches roughly the localized resonance condition.

--From: "Plasmonic Optics: Theory and Applications" By Yongqian Li, SPIE Press, 2017, p.79

其中，V表示金属纳米球的体积。方程（1-48）表明，如果金属的复介电函数的虚部对入射光频率依赖性很小时，则发生 LSP 共振的条件$\varepsilon_1(\omega) = -\chi\varepsilon_d(\omega)$。对于半径较小的球体和球状体，$\chi$的值近似于 2；对于椭球纳米粒$\chi$的值近似等于 3。因此，对较小的纳米球发生 LSP 共振条件是$\varepsilon_1(\omega) = -2\varepsilon_d(\omega)$。从表达式（1-46）、（1-47）和（1-48）可以看出，散射、吸收和消光系数与金属纳米结构的尺寸、材料和所处环境有密切相关。

--来源于："金属手性微纳结构的非对称传输与圆二色性研究"，吐达洪·阿巴，陕西师范大学，2020 年，第 16 页

第 17 段

2.1.4 Momentum mismatch

When $|\varepsilon'_m| \gg \varepsilon''_m$, the imaginary part of metallic media in Eq. (2.17b) is neglected. In the ideal case of free electron gases, the dielectric function of a bulk metal is derived from the Drude model as

$$\varepsilon_m = 1 - \omega_p^2/\omega^2. \tag{2.25}$$

Equation (2.25) is substituted into Eq. (2.15), and the dispersion relation of SPPs becomes

$$k_x = k_{sp} = \frac{\omega}{c}\sqrt{\frac{\varepsilon_d\varepsilon_m}{\varepsilon_d + \varepsilon_m}} = \frac{\omega}{c}\sqrt{\frac{(\omega^2 - \omega_P^2)\varepsilon_d}{(1+\varepsilon_d)\omega^2 - \omega_P^2}}. \tag{2.26}$$

In the case of $\varepsilon_m \to -\varepsilon_d$, the value from Eq. (2.26) approaches an infinitely increasing value $k_x \to \infty$. The corresponding angular frequency tends to a horizontal asymptotic value of

$$\omega \equiv \omega_{sp} = \frac{\omega_p}{\sqrt{1+\varepsilon_d}}. \tag{2.27}$$

The permittivity of the vacuum medium approaches 1 as the wave vectors become larger, which leads to the possible asymptotic frequency

$$\omega_{sp} \approx \omega_p/\sqrt{2}. \tag{2.28}$$

Thus, the energy of the surface plasmon wave becomes independent of the incident wave vector. SPPs could then be excited by an electromagnetic wave with a frequency below the bulk plasmon frequency. The frequency range of the surface plasmon is $\omega_{sp} = 0 \sim \omega_p/\sqrt{2}$.

--From: “Plasmonic Optics: Theory and Applications” By Yongqian Li, SPIE Press, 2017, p.47-48

一般可以将贵金属中的传导电子近似看作为经典的理想气体模型，从而得到经典的自由电子气体理论。因此，金属的介电常数用以

下方程表示[58]:

$$\varepsilon_m(\omega) = 1 - \omega_p^2/\omega^2, \tag{1-49}$$

其中ω_p表示金属的等离子体频率。将方程 (1-49) 代入方程 (1-30)，可推导包含等离子体频率的 SPP 色散关系表示为

$$k_{sp} = \frac{\omega}{c}\sqrt{\frac{\varepsilon_d\varepsilon_m}{\varepsilon_d+\varepsilon_m}} = \frac{\omega}{c}\sqrt{\frac{(\omega^2-\omega_p^2)\varepsilon_d}{(1-\varepsilon_d)\omega^2-\omega_p^2}}。 \tag{1-50}$$

当$\varepsilon_m \to -\varepsilon_d$时，在方程（1-50）中，$k_{sp} \to \infty$，如图 1-10 所表示，则相应的角频率趋向于水平的渐近值为

$$\omega \equiv \omega_{sp} = \omega_p/\sqrt{1+\varepsilon_d}。 \tag{1-51}$$

当取空气的介电常数为$\varepsilon_d = 1$时，则 SPP 和等离子体频率关系表示为

$$\omega_{sp} \approx \omega_p/\sqrt{2}。 \tag{1-52}$$

--来源于：“金属手性微纳结构的非对称传输与圆二色性研究”，吐达洪·阿巴，陕西师范大学，2020 年，第 16-17 页

第 **18** 段

On the other hand, for low frequencies, the dielectric permittivity of metallic materials approaches infinite values, and Eq. (2.15) evolves into the dispersion relation of light propagating in an air medium:

$$k_x = \frac{\omega}{c} \lim_{\varepsilon_m \to -\infty} \sqrt{\frac{\varepsilon_d \varepsilon_m}{\varepsilon_d + \varepsilon_m}} \approx \frac{\omega}{c} \sqrt{\varepsilon_d}, \tag{2.29}$$

which overlaps with the light line of the air medium. The dispersion relations of SPPs are shown in Fig. 2.3. For small wave-vector values, the dispersion curve approaches but is always lower than the light line. The region on the left side of the light line is called the radiative region, as denoted by the shaded area, which covers the dispersion curves of electromagnetic waves propagating in the air medium.

The transverse component of the incident wave vector is identified as k_{in}. The region to the right of the light line is the nonradiative region, where the surface plasmon dispersion curve exists. A surface plasmon wave belongs to the nonradiative modes. The curve of the surface plasmon mode keeps to the right of the light line and never interacts directly with that of the electromagnetic wave in air. A momentum deviation G exists between the surface plasmon mode and free space lights at the same frequencies. The momentum gap becomes greater with the increasing frequency. The incident wave therefore would not be coupled directly into the surface plasmon mode, which implies that the SPPs cannot be excited directly by an incident wave.

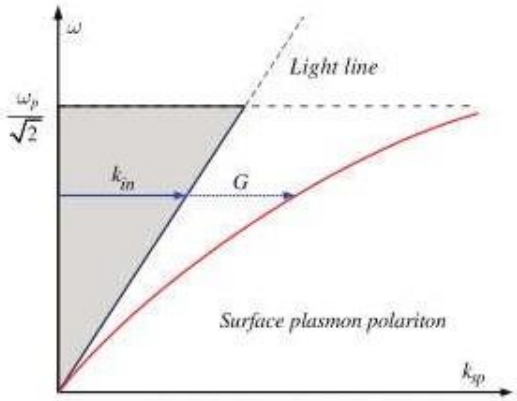

Figure 2.3 Dispersion relations of SPPs. The dotted light line represents the dispersion relation for light in vacuum.

In order to make up for this momentum mismatch, an additional momentum is necessary to cover the momentum deviation between the incident wave vector k in and the surface plasmon mode k_{sp} . The wave vector condition is

$$k_{sp} = k_{in} + G \tag{2.30}$$

--From: “Plasmonic Optics: Theory and Applications” By Yongqian Li, SPIE Press, 2017, p.48-49

在导体和介质的二维界面上传播的 SPP 本质上是平面电磁波。由于 SPP 的传播波矢量k_{SPP}总是大于光在介质中的波矢量k_0，即$k_{SPP} > k_0$，所以其被束缚在界面附近，而且在传播时将在界面两侧发生衰减，如 1-7 所示。假设入射电磁波波矢量的横向分量标识为k_0，如图 1-10 所表示的金属/空气界面上 SPPs 的色散曲线（SPPs dispersion curve）图，光线（light line）右侧的区域是非辐射区域，其包含 SPP 色散曲线[59]。SPP 波属于非辐射的电磁波。SPP 模式色散曲线在光线的右边，并且一般不能直接自然地与空气中的电磁波波矢量相互交叉，从而在相同频率的 SPP 模式和自由空间的光之间存在动量 G 偏差。如图 1-10 所示，动量差异随着频率的增加而变大。因此，入射光的光子不会直接耦合到 SPP 模式，这意味着入射波不能直接激发 SPP 模式。同时，根据表达式（1-52），SPP 的色散曲线不能大于水平的渐近值，这说明想要激发 SPP 波必须需要另外补充动量 G，则用外来动量或者补偿方式来实现匹配入射波矢量k_0和 SPP 波矢量k_{sp}之间的动量色散关系，即匹配的波矢条件表示为，

$$k_{sp} = k_{in} + G \tag{1-53}$$

其中，k_{in}是入射光的波矢量，G 另外需要的附加动量。如图 1-10 所示，SPP 波矢量和自由空间中的电磁波波矢量之间存在动量差异，自

由空间中的电磁波不能在电介质和金属界面上直接激发 SPP 波，要想真空中的光子动量与金属/空气界面的 SPPs 动量匹配，必须通过某种方式提供一个附加动量。为实现动量匹配，需要提高激发光的动量[59]，如图 1-11 所示，研究发现，激发 SPP 波的最常用的方法有：棱镜耦合、光栅耦合、强聚光束激发和近场激发等。

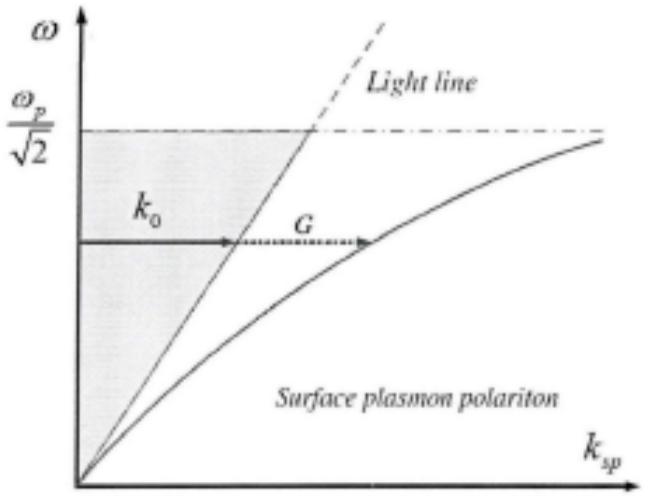

图 1-10 SPPs 色散曲线；虚线表示光在真空中的色散关系[44]

--来源于："金属手性微纳结构的非对称传输与圆二色性研究"，吐达洪·阿巴，陕西师范大学，2020 年，第 16-17 页

第 19 段

The prism-coupling approach, also known as the attenuated total reflection (ATR) method, is the well-known Kretschmann configuration, as shown in Fig. 2.12(a). In this solution, an incident wave illuminates the metal film through the dielectric prism, which creates an evanescent wave at the interface between an optical density medium and a metallic medium.

The continuity boundary conditions enable the wave vector in the prism to coincide with the SPPs at the metal–dielectric surface, which results in the excitation of the SPPs. 15 The wave vector of the excited SPPs is described by Eq. (2.43), which includes the functions of the incident angle and the frequency of the incidence electromagnetic wave. It is rewritten here as

$$k_x = k_0\sqrt{\varepsilon}\,sin\,\theta, \tag{2.46}$$

where ε p refers to the permittivity function of the prism material. Equation (2.46) implies that there are two approaches to excite a surface plasmon mode. For incident light with a fixed wavelength, a variety of incident angles can excite SPPs throughout the dispersion curve. This excitation method is called the angle-scanning method. During this process, an evanescent wave is coupled to the form of the SPPs; part of the light reflects back into the prism, and part refracts out the prism.

--From: “Plasmonic Optics: Theory and Applications” By Yongqian Li, SPIE Press, 2017, p.57-58

棱镜耦合法，也称为衰减总反射法，也就是典型的 Kretschmann 结构。由于金属与介质的平面上 SPP 波矢量k_{SPP}大于光在电介质交面上的波矢量k_0，所以不能由光束直接激发出来。同时以θ角入射的光波矢量在平面界面上的投影分量$k_x = k_0\,sin\,\theta$也总小于 SPP 的波矢量k_{SPP}，无法实现相位匹配。然而，在一个两层具有不同介电常数的介质夹着一层金属薄膜的三层结构中，可以实现 SPP 的波矢匹配，如图

1-11（a）所示。通常在棱镜与金属界面发生反射时，完全足够激发位于金属与低介电常数材料界面的 SPP，即金属与空气界面上的 SPP，其中金属面内动量为$k_x = k_0\sqrt{\varepsilon}\,sin\,\theta$。在棱镜耦合激发方法中，入射光通过介质为$\varepsilon_p$的棱镜照射在金属薄膜上，棱镜在光密度介质和金属介质的界面处产生一个倏逝波（evanescent wave），连续的边界条件使得棱镜中的波矢量与金属-介质界面上的 SPP 一致。当在空气和高介电常数介质界面区域时，满足动量匹配时入射光可以激发 SPP 波。

--来源于："金属手性微纳结构的非对称传输与圆二色性研究"，吐达洪·阿巴，陕西师范大学，2020 年，第 18 页

第 **20** 段

In order to overcome the thickness problem, the **Otto** geometry has been proposed. As shown in Fig. 2.13(b), an air gap replaces the dielectric layer. The thickness of the air gap is tens of nanometers, which ensures the realization of the resonant conditions[16].

--From: "Plasmonic Optics: Theory and Applications" By Yongqian Li, SPIE Press, 2017, p.59

而奥托结构（**Otto**）的激发原理是棱镜与金属薄膜之间存在很窄的空气隙缝，空气与棱镜的界面发生全内反射，部分光子隧穿到空气与金属的界面激发 SPP 波[60]。

--来源于："金属手性微纳结构的非对称传输与圆二色性研究"，吐达

洪·阿巴，陕西师范大学，2020 年，第 818 页

第 **21** 段

The grating excitation method is one frequently used technique in plasmonic optics, in which periodic nanostructures are introduced to eliminate the momentum mismatch of the wave vectors. 17,18 As shown in Fig. 2.14(a), the diffracted orders of the periodically corrugated interface exhibit larger wave-vector magnitudes than those of incident waves. For a 1D grating, the condition for the excitation of the SPPs is

$$k_{spp} = k_{in} \sin\theta_{in} \pm m\frac{2}{p} \qquad (2.47)$$

where p refers to the lattice constant, and m = (1, 2, . . .) is the order of diffracted wave component. The grating provides wave vector compensation m × 2π/p to the incident wave $k_{x,in} = k_{in} \sin\theta$ in along the propagation direction, which compensates for the deficiency between k_{sp} and $k_{x,in}$. The mismatch compensation by the grating excitation method is indicated in Fig. 2.14(b).

--From: “Plasmonic Optics: Theory and Applications” By Yongqian Li, SPIE Press, 2017, p.59-60

光栅耦合激发方法是在 SPP 激发中常用的一种方法，它的原理是通过引入周期性的纳米结构来实现动量匹配[61]。如图 1-11（b）所示，通过金属凹槽光栅来，可以激发 SPP 波的条件是

$$k_{spp} = k_{in}\, sin\, \theta_{in} \pm m\frac{2}{p} \quad (1\text{-}54)$$

制作光栅常数为 p 的凹槽或者孔洞光栅来实现 SPP 波的激发。这里，p 是光栅常数，m = (1,2,….) 是衍射波的级数。光栅为沿着$k_{x,in} = k_{in}\, sin\, \theta_{in}$方向的入射光提供了以$m\frac{2}{p}$的矢量补偿，使得$k_{SPP}$和$k_{in}$之间的矢量发生匹配。与棱镜耦合方法一样，当检测到反射光谱中出现最小值时，说明激发了 SPP 波。它的优势在于耦合效率强、技术要求较低且便于操作。因此光栅耦合方法降低了激发 SPP 的技术难度，提供了广泛应用的激发方法。

--来源于："金属手性微纳结构的非对称传输与圆二色性研究"，吐达洪·阿巴，陕西师范大学，2020 年，第 18-19 页

第 **22** 段

Both the prism excitation and grating excitation method offer standard methods to excite nonradiative surface plasmon polaritons. However, it is rather difficult for these configurations to miniaturize the excitation systems. Fortunately, near-field excitation techniques can make up for this deficiency.

Near-field optical techniques provide the potential tools for plasmonics optics to excite surface plasmon polaritons in integrated photonic devices. 17,21 As shown in Fig. 2.15, the diffraction effect of a probe tip and the scattering effect of a surface bulge are often used to compensate for a momentum mismatch. The diffractive effects from these corrugated metal–

dielectric nanostructures stimulate a variety of SPP modes.

In the configuration of a probe tip, the incident light through a small probe tip illuminates the metal film surface. Because of the concentration effect ascribed to the small aperture size, the exiting waves from the tip aperture satisfy the condition of $k_{tip} < k_{sp} < k_0$. Then circular expanding waves of SPPs can be locally achieved at the surface.

--From: "Plasmonic Optics: Theory and Applications" By Yongqian Li, SPIE Press, 2017, p.60-61

虽然，棱镜耦合法和光栅耦合法都为激发非辐射SPP提供了一个比较理想的方法，但是棱镜和光栅等结构对系统的小型化又带来了很大的困难。然而，近场激发法可以弥补这一不足。近场光学显微镜技术能够在一个非常小的区域内激发局部的SPP，并且看作一个SPP的电源。近场光学技术为集成光子器件中的SPP激发提供了潜在的工具[64]。它的原理是使用凸起的针尖来实现动量匹配。这些波纹状金属电介质纳米结构的衍射效应和散射效应激发了各种SPP模式。如图1-11 (d) 所示，a表示探针长度，一个尺寸为$a \leq \lambda_{spp} \leq \lambda_0$的针尖 (Tip) 在近场范围照射金属膜面，由于探针孔径尺寸很小，从针尖发出的光包含波矢分量$k_{tip} \geq k_x \geq k_0$，这样能够实现波矢$k_x$的SPP相位匹配激发。近场激发方法为单个纳米结构进行光谱分析提供一个可行的技术手段。

--来源于："金属手性微纳结构的非对称传输与圆二色性研究"，吐达

洪·阿巴，陕西师范大学，2020 年，第 20 页

第 **23** 段

The obvious difference between the optical responses of metals and dielectrics enables them to be fundamental elements for designing plasmonic devices. In plasmonic optics, metals are incorporated into nanostructures for the emerging characteristics of the SPPs and other light–matter interactions. This section emphasizes the optical performance of metals following the theory model for free electrons and bound electrons, pursing the approach for realizing the optimal plasmonic materials at the nanoscale.

--From: “Plasmonic Optics: Theory and Applications” By Yongqian Li, SPIE Press, 2017, p.15

金属和电介质的光学响应之间的明显差异，是它们设计各种等离激元器件的基本元素。在 SP 中，由金属和电介质结合组成的微纳结构显示了 SPP 特征和增强光-物质相互作用。本节根据自由电子和束缚电子的理论模型强调金属的光学性能，并对在纳米级实现最佳 SP 材料的微**观电子电子动**力学理论中研究出的 Drude-Lorentz 模型进行简介[91]，最后用它来解释金属材料的光学特性。

--来源于：“金属手性微纳结构的非对称传输与圆二色性研究”，吐达洪·阿巴，陕西师范大学，2020 年，第 34-35 页

第 **25** 段

As shown in Fig. 1.5, a charge within a medium is treated as a harmonic oscillator, which is bounded with a nucleus. Under the excitation of an incident electromagnetic wave, the oscillator will oscillate in the oppositional phase relative to the electric field. Here, only the conditions of a nonpolar molecule are discussed, in which no dipole moment exists in the electron–nucleus system. From the dynamic point of view, the charge oscillation will lead to the charge redistribution, which will create an additional induced electric field. The induced field will restore the charge to its equilibrium position. Newton's second law states that the production of mass multiplying the acceleration equals the sum of the forces applied on the system. The governing equation for the system in Fig. 1.5 is

$$m_e \frac{\partial^2 \vec{r}(t)}{\partial^2 (t)} = q_e E_{in} e^{-j\omega t} + [-q \times \vec{r}(t)] + [-\gamma[\partial \vec{r}(t)/\partial t]]$$

where me denotes the effective mass of a charge, r(t) is the instantaneous distance deviation from its equilibrium position. $q_e E_{in} e^{-j\omega t}$ is the local force attributed to an external alternating electric field, where q e is the electric quantity of an charge, and E0 is the electric field amplitude. $-q \times \vec{r}(t)$ is the restoration force proportional to the distance deviation from the equilibrium position $q = m_e \omega^2$, where ω^2 is the natural frequency of the bound oscillator. The restoration forces are zero for free electrons within conductor materials because they are not bound to a

particular nucleus. $F_D = -\gamma[\partial r(t)/\partial t]$ refers to the damping force due to the collision energy loss, γ where g is the damping coefficient in hertz.

Note that the restoration and damping forces are negative because they are opposite the direction of the motion. Thus, the differential form in Eq. (1.41) becomes:

$$m_e \frac{\partial^2 \vec{r}}{\partial^2 t} + m_e \gamma \frac{\partial \vec{r}}{\partial t} + m_e \omega_0^2 \vec{r} = q_e E_{in} e^{-j\omega t}$$

The interactions between metals and electromagnetic waves are firstly determined by the collective movement of free electrons. In this case, the electrons are not bound to any particular nucleus, which are considered to move about freely around the metal lattice in the absence of a restoration force. The motion equation of a free electron in an alternating electric field is described by

$$m_e \frac{\partial^2 \vec{r}}{\partial^2 t} + m_e \gamma \frac{\partial \vec{r}}{\partial t} = -q_e E_{in} e^{-j\omega t}$$

where q e is the electric charge of a free electron. the damping effect g is proportional to the Fermi velocity g ¼ n/l¼ 1/t, where n denotes the Fermi velocity, and l is the mean free path of an electron between successive collision events. The relaxation time t is the averaged interval time between subsequent collisions of an electron. In general, the relaxation time is about 10 –14 s. The solution of instaneous distances in Eq. (1.49) for a monochromatic electric field is solved to be

$$\vec{r}(\omega) = \frac{q_e}{m_e(\omega^2 + j\gamma\omega)}\vec{E}_{in}(\omega) \qquad (1.50)$$

The polarization density is the total dipole moment per unit volume. The gross polarization of all of the electrons in the unit volume is

$$\vec{P} = \frac{Nq_e^2}{m_e(\omega_0^2 + j\gamma\omega)}\vec{E}_{in}(\omega) \qquad (1.51)$$

where N is the electron density per unit volume. A comparison of Eqs. (1.45) and (1.51) leads to the frequency-dependent permittivity of metals as

$$\varepsilon(\omega) = 1 - \frac{\omega_p^2}{\omega^2 + j\gamma\omega} \qquad (1.52)$$

where v p is the plasma frequency of the bulk media, which has a similar physical mechanism as the definition in Eq. (1.47). At the plasma frequency, the electromagnetic response of a material changes from the metallic behaviors to those of dielectric materials.

--From: “Plasmonic Optics: Theory and Applications” By Yongqian Li, SPIE Press, 2017, p.17-19

通常，利用物理模型描述固体材料与电磁场作用的介电特性。如图 2-4 所示，假设，将金属中的电荷看作以原子核为界的谐振子，则它在入射光的激励下，振荡器相对于电场以相反的相位进行振荡。假定，该谐振子是非极性分子的条件，

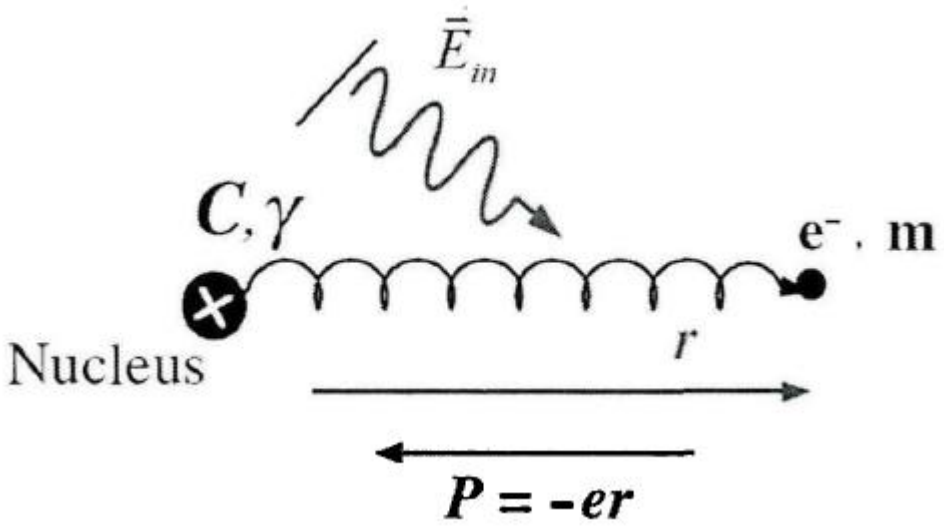

图 2-4 外加电场中谐振子模型的电子运动示意图[92]。

Fig. 2-4 Schematic of electron motion for a harmonic oscillator model in an external electric field.

则在电子-原子核系统中没有偶极矩存在。从动力学角度看，电荷振荡会使电荷重新分布，从而产生额外的感应电场，感应电场将使电荷恢复到平衡位置。牛顿第二定律指出，质量加速度的乘积等于作用在系统上的力之和，因此，该系统的动力学方程可以表示为[92]

$$m_e \frac{\partial^2 \vec{r}(t)}{\partial^2 (t)} = q_e E_{in} e^{-j\omega t} + [-q \times \vec{r}(t)] + [-\gamma[\partial \vec{r}(t)/\partial t]], \quad (2\text{-}15)$$

其中，右边的第一第二第三项分别表示外加电场产生的局部力、感应电场产生的恢复力和碰撞能量损失而引起的阻尼力。m_e是电荷有效质量，$\vec{r}(t)$是偏离其平衡位置的瞬时距离，q_e是电荷量，E_{in}入射电场振幅，$q = m_e \omega_0^2$是平衡位置，在这里，ω_0是振荡器的固有频率，

γ是以赫磁为单位的阻尼系数。恢复力和阻尼力均为负，因为它们与运动方向相反。因此，等式(1-1)中的微分形式整理可写为

$$m_e \frac{\partial^2 \vec{r}}{\partial^2 t} + m_e \gamma \frac{\partial \vec{r}}{\partial t} + m_e \omega_0^2 \vec{r} = q_e E_{in} e^{-j\omega t}。 \quad (2\text{-}16)$$

假设在没有恢复力的情况即$m_e \omega_0^2 \vec{r} = 0$，则金属和电磁波之间的相互作用取决于自由电子气的集体运动。在这种情况下，电子$(-q_e)$不与任何特定的原子核结合，电子可被认为在金属晶格周围自由移动。那么自由电子在交变电场中的运动方程可表示为

$$m_e \frac{\partial^2 \vec{r}}{\partial^2 t} + m_e \gamma \frac{\partial \vec{r}}{\partial t} = -q_e E_{in} e^{-j\omega t}, \quad (2\text{-}17)$$

其中，q_e式自由电子的电荷量，v是费米速度，τ是自由电子弛豫时间，一般弛豫时间大概$10^{-14}s$，阻尼效应γ和费米速度成正比，即$\gamma = v/\tau$。假设入射电场是单色电场，则方程(1-17)的瞬时解析为

$$\vec{r}(\omega) = \frac{q_e}{m_e(\omega^2 + j\gamma\omega)} \vec{E}_{in}(\omega)。 \quad (2\text{-}18)$$

单位体积中所有电子的总极化可表示为$\vec{P} = N q_e \vec{r}(\omega)$，其中$N$是单位体积中电子密度，$\omega$是入射光的角频率。极化密度是每单位体积的总电偶极矩。将式(2-18)代入总极化式子，可推得到

$$\vec{P} = \frac{N q_e^2}{m_e(\omega_0^2 + j\gamma\omega)} \vec{E}_{in}(\omega) \quad (2\text{-}19)$$

由极化密度与入射电场之间的关系式，可写成为：

$$\vec{P} = \varepsilon_0(\varepsilon_r - 1)\vec{E}_{in}(\omega) \quad (2\text{-}20)$$

由表达式(1-7)和(2-20)结合可得到金属的频率相关的复介电函数[92]

$$\varepsilon(\omega) = 1 - \frac{\omega_p^2}{\omega^2 + j\gamma\omega}, \tag{2-21}$$

这里，ω_p是块体金属的等离子体频率，并$\omega_p^2 = \frac{N_e q_e^2}{m_e \varepsilon_0}$。表达式(2-21)描述自由电子气复介电函数，又称为金属材料光学响应的经典的德鲁特（Drude）模型。当入射光的角频率和金属的等离子体频率相等时，即$\omega = \omega_p$，材料的电磁响应从金属行为变为电介质材料，相当于没任何响应。当$\omega < \omega_p$时，介质的光学特性表现出金属的行为。当$\omega >> \omega_p$时，材料的光学性质表现出电介质的属性。

--来源于："金属手性微纳结构的非对称传输与圆二色性研究"，吐达洪·阿巴，陕西师范大学，2020 年，第 35-36 页

第 26 段

Equation (1.52) describes the contribution of free electrons to the permittivity of metals. The permittivity in Eq. (1.52) is rewritten into the real and imaginary parts

$$\varepsilon(\omega) = (1 - \frac{\omega_p^2}{\omega^2 + \gamma^2}) + j\frac{\gamma\omega_p^2}{\omega(\omega^2 + \gamma^2)} \tag{1.53}$$

In the conditions of v .. g, Eq. (1.53) is simplified to be

$$\varepsilon\ \ (\omega) \approx 1 - \frac{\omega_p^2}{\omega^2} + j\frac{\gamma\omega_p^2}{\omega^3}\gamma \tag{1.54}$$

The permittivity of metal gold is calculated by Eq. (1.53), ranging from visible to infrared wavelengths. As shown in Fig. 1.6, the real part of the

permittivity for metal gold remains negative throughout the wavelengths in which the frequencies are less than the plasma frequency. The negative permittivity results in an imaginary part of the refractive index. For metals, the imaginary part of the permittivity implies an energy dissipation that is relevant with the thermal motion of electrons.

Figure 1.6 indicates that, in the infrared wavelengths longer than ?650 nm, the Drude model gives an accurate permittivity of gold, and the experimental data clearly agree well with the Drude theory. However, there is an obvious deviation of the imaginary part in the visible wavelengths shorter than 650 nm. The measured imaginary part increases much more sharply than that predicated by the Drude theory. This difference is attributed to the fact that the interband transitions of the bound electrons excited by the photons .

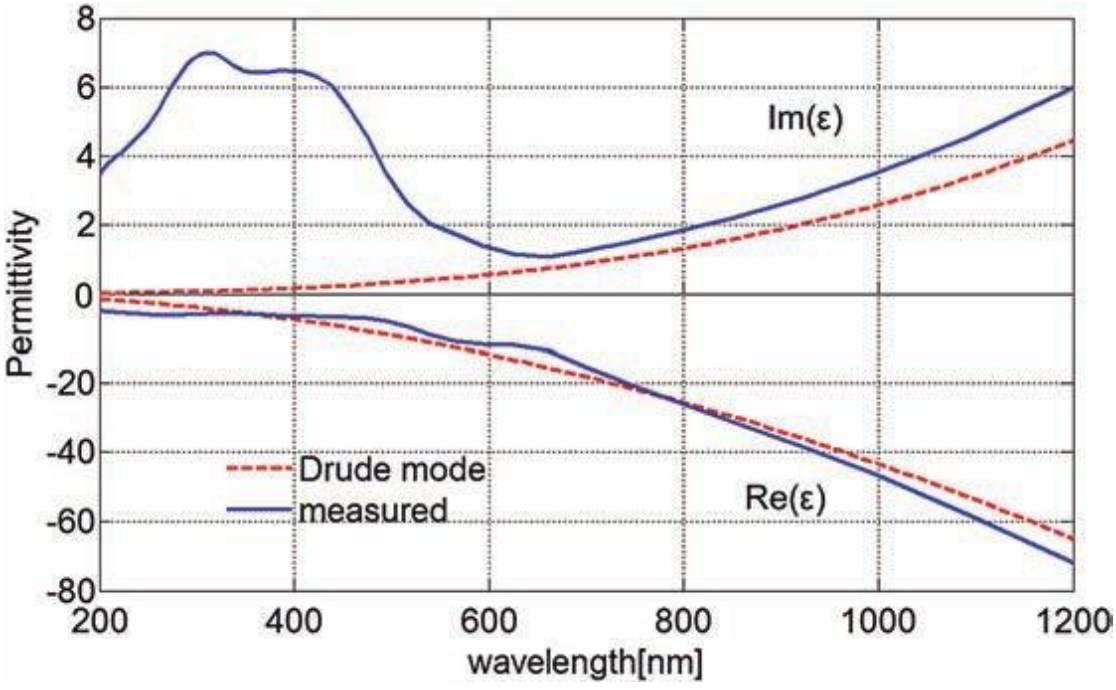

Figure 1.6 Permittivity of metal gold estimated by the Drude model (dotted line) and the measurement (solid line). The measured data come from Ref. [10]. The parameter values in the Drude model are adopted from Table 1.2.

with higher energy have not been taken into account in the Drude model, where, however, the interband transitions become significant. The contribution from the interband transitions ofbound electrons to the dielectric permittivity looks like the corresponding resonance in dielectric media. These transitions are obtained from the governing equations without consideration of the free electrons as

$$\varepsilon(\omega) = 1 + \sum_i^K \frac{f_i \omega_i^2}{\omega_i^2 - \omega^2 - j\gamma_i \omega} \qquad (1.55)$$

where w0 is the oscillation frequency of a bound electron under an electric field, and w1 and g are related to the corresponding frequency and damping of a bound electron, respectively.

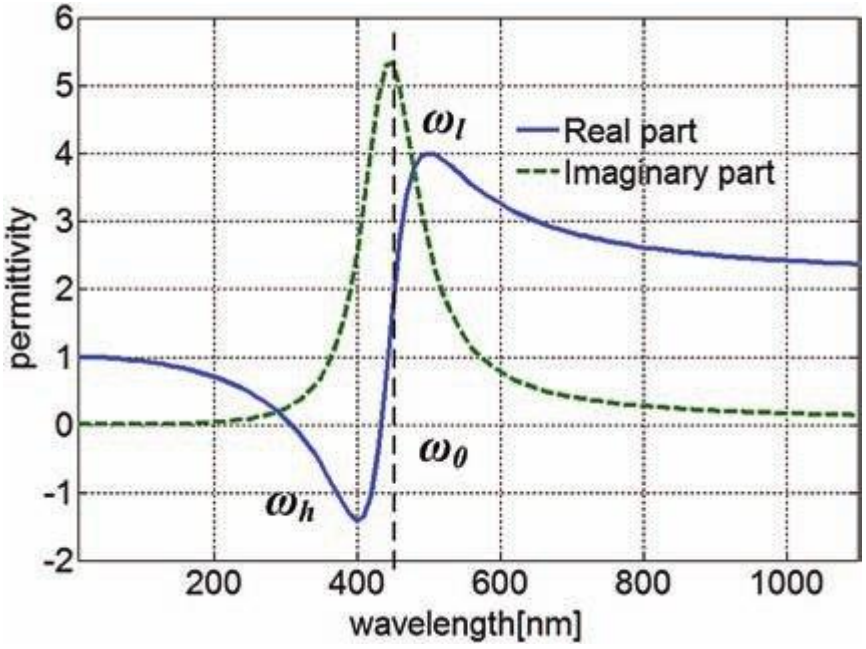

Figure 1.7 Contribution of the bound electrons in metal gold to the permittivity. The values of the parameters used are v 1 ¼ 4.55 ? 10 15 s ?1 , g ¼ 9.10 ? 10 16 s ?1 . The central resonance wavelength is 450 nm (v 0 ¼ 4.19 ? 10 17 s ?1).

Figure 1.7 shows the dielectric permittivity of metal gold considering only the interband contribution of bound electrons. The real part shows a dispersion behavior while the imaginary part displays a clear resonant behavior. The vertical dotted line represents the resonant frequency v 0 that is consistent with the zero value of the second part on the right side of Eq. (1.52). The resonant frequency w0 also agrees well with the peak value of the imaginary part, so it is sometimes called the absorption frequency. For the real parts, there is a peak value in the lower frequency and a valley value in the higher frequency that is greater than the resonant frequency. The frequency region between the mal dispersion region, where the

permittivity values decrease with the increasing frequency. For a Lorentz oscillator, the real part of permittivity is a positive value in the range less than the resonance frequency, while there is a negative valley at the slightly higher frequency than the resonance frequency. Another feature in Fig. 1.7 is that the dielectric permittivity has a nonzero asymptotic value when the wavelength increases much longer than the resonance wavelength. After all, if the interband electron transitions within media have been taken into account, such an asymptotic constant should approach one summary value[11].

If the higher order of interband electrons transition is taken into account the dielectric permittivity is expressed as the model superposition of the Lorentz model as

$$\varepsilon(\omega) = 1 - \frac{\omega_p^2}{\omega^2 - j\gamma_d\omega} + \sum_i^K \frac{f_i\omega_i^2}{\omega_i^2 - \omega^2 - j\gamma_i\omega}$$

where i refers to the resonant modes, wi corresponds to the resonance frequencies, fi indicates the weighting coefficients, and γ_i is the damping effect.

--From: “Plasmonic Optics: Theory and Applications” By Yongqian Li, SPIE Press, 2017, p.20-22

方程(1-21)描述了自由电子对金属介电常数的贡献，这说明金属只有在特定频率范围内与入射光发生强烈作用，金属的光学效应依赖

于入射光的频率，即它是入射光的函数。在表达式（2-21）中，块体金属的复介电函数由实部和虚部两部部分组成，即$\varepsilon(\omega) = \varepsilon_1 + j\varepsilon_2$，此虚部和实部可以由下式表达为

$$\varepsilon(\omega) = (1 - \frac{\omega_p^2}{\omega^2+\gamma^2}) + j\frac{\gamma\omega_p^2}{\omega(\omega^2+\gamma^2)}。 \quad (2\text{-}22)$$

当$\omega >> \gamma$时，方程(2-22)可以简写为

$$\varepsilon\ (\omega) \approx 1 - \frac{\omega_p^2}{\omega^2} + j\frac{\gamma\omega_p^2}{\omega^3}\gamma。 \quad (2\text{-}23)$$

在方程式（2-21）中的金属的复介电函的效应数范围从可见光到红外波长。在大于 650 nm 的红外波长中，Drude 模型能够给出精确的金属复介电函数，如图 2-5（a）所示，这时实验数据与 Drude 理论非常一致[93]。然而，在小于 650 nm 的可见波长中，虚部有明显的偏差。这时测得的虚部值比 Drude 理论预测的虚部值增加还多，两条曲线不大吻合。这种差异归因于 Drude 模型中并未将具有较高能量的光子激发的束缚电子带间跃迁考虑进去。可是，在小于 650 nm 可见光区域，带间跃迁影响很大，因此，在实际的实验中只有将这因素考虑进去时，结果才符合客观事实。

金属材料的 Lorentz 模型正好完善了这一不足。如图 2-5（b）显示，它考虑到金属的介电常数仅束缚电子的带间贡献。实部曲线显示色散行为，而虚部显示出明显的共振行为。共振频率ω_0与虚部曲线的峰值也非常吻合，因此这种行为称为吸收频率。对于金属材料实部来说，低频段有一个峰值ω_l，高频段有一个谷值ω_h，并大于共振频率ω_0，

两个极值之间的频率区域称为异常色散区域，其中复介电常数值随频率增加而减小。

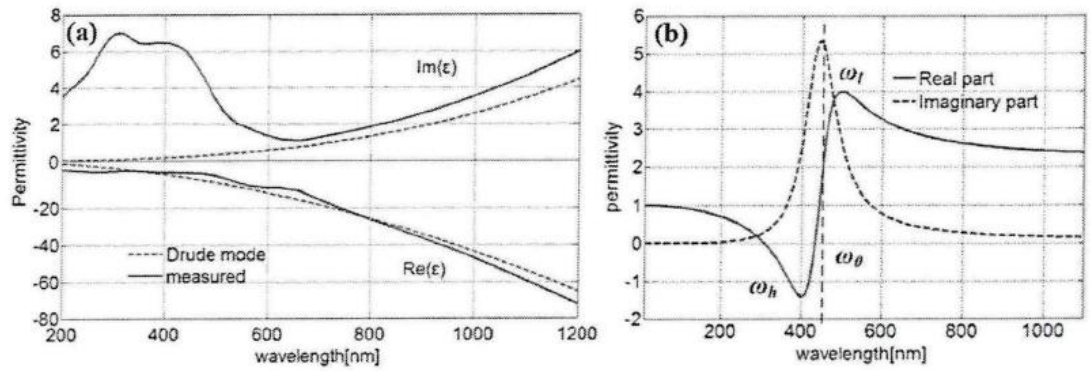

图 2-5 金属材料的介电常数曲线[58]。(a) 由 Drude 模型（虚线）和测量值（实线）下得到的介电常数曲线；(b) 考虑金属中的束缚电子的贡献时的介电常数曲线。

Fig.2-5 Permittivity of metal material. (a) permittivity of metal gold estimated by the Drude model (dotted line) and the measurement (solid line); (b) contribution of the bound electrons in metal gold to the permittivity.

对于洛伦兹（Lorentz）振荡器，介电常数的实部在小于谐振频率的范围内为正值，而在比谐振频率稍高的频率处存在负谷。如图 2.5（b）所示，当波长增加远大于共振波长时，介电常数具有非零的渐近值。如果考虑高阶的带间电子跃迁，则介电常数表示为 Lorentz 模型的模型叠加[58]，即

$$\varepsilon(\omega) = 1 + \sum_i^K \frac{f_i \omega_i^2}{\omega_i^2 - \omega^2 - j\gamma_i \omega}, \tag{1-24}$$

其中，i表示谐振模式，ω_i是相应的谐振频率，f_i是加权系数，γ_i是

阻尼效应。假定每个电子都有助于偶极极化。因原子核的质量比电子的质量大得多，原子核也起到了一部分作用，但是可以把这点微小的作用忽略不计。在 Drude 模型的复介电常数中上述公式是在无限核质量近似的条件下得出的。另外一个假设是在一个电子动力学系统中只有一个电子起作用，一般束缚电子和自由电子都对金属介质的光学性质有贡献。因此，结合带内效应的 Drude 分量和带间跃迁的 Lorentz 项，可以得到更接近描述真实金属材料的复介电常数的较完整的 Drude-Lorentz 模型[94]，

$$\varepsilon(\omega) = 1 - \frac{\omega_p^2}{\omega^2 - j\gamma_d\omega} + \sum_i^K \frac{f_i\omega_i^2}{\omega_i^2 - \omega^2 - j\gamma_i\omega}, \quad (1\text{-}25)$$

其中，K表示对应于共振ω_j的高阶谐振子的总数，γ_d是阻尼常数，$\frac{1}{\gamma_j}$是共振寿命。当更多的带间跃迁被整合到表达式（1-25）中时，计算数据和实验数据较为接近。这样以来，修正后的 Drude-Lorentz 模型可以弥补 Drude 模型中的不足，近似地描述真实金属材料的光学特性。在本文的研究中，使用修正后的金属 Drude-Lorentz 模型的复介电函数来进行科学研究工作。

--来源于：“金属手性微纳结构的非对称传输与圆二色性研究”，吐达洪·阿巴，陕西师范大学，2020 年，第 36-38 页